Reprint from

OPHELIA

International Journal of Marine Biology

VOL. 41

OPHELIA PUBLICATIONS

MARINE BIOLOGICAL LABORATORY, HELSINGØR, DENMARK

1995

OPHELIA 41: 5-36 (February 1995)

ECOLOGICAL MODELLING IN COASTAL WATERS: TOWARDS PREDICTIVE PHYSICAL-CHEMICAL-BIOLOGICAL SIMULATION MODELS

Dag L. Aksnes[1], Kåre B. Ulvestad[1], Beatriz M. Baliño[1], Jarle Berntsen[2], Jorun K. Egge[1] & Einar Svendsen[3]

[1]Department of Fisheries and Marine Biology, University of Bergen, Høyteknologisenteret, N-5020 Bergen, Norway

[2]Department of Mathematics, University of Bergen, Allégt. 55, N-5007 Bergen, Norway

[3]Institute of Marine Research, P.O. Box 1872 Nordnes, N-5024 Bergen, Norway

ABSTRACT

A simple, but general, simulation model is specified according to the state-of-the-art within phytoplankton modelling: Process representations are based upon prevailing theoretical and empirical representations given in the literature, and a set of earlier published values of model coefficients that have demonstrated good fit to reliable observations was selected. The emerging phytoplankton model was then validated against data obtained from enclosure experiments with light-, N-, P- and Si-limitations. We applied no tuning of the coefficients as the purpose of this test was to estimate the predictive power of the proposed model. The general standard deviations between model predictions and observations were on the range 0.04-0.36 and 0.13-0.42 for the nutrient and phytoplankton state variables respectively. Not surprisingly, these values are higher than those obtained in tuned simulations. Nevertheless, several characteristics, such as the balance between diatoms and flagellates, were predicted by the model. The phytoplankton model was set up and driven by a 3-dimensional physical model for the North Sea. The period February-June 1988 was simulated and forced with realistic topography, meteorological data, riverine freshwater and nutrient input. Simulated developments in nutrients, diatoms and flagellates are presented with references to actual observations and the *Chrysochromulina polylepis* bloom in 1988. Several important characteristics, such as the timing of two diatom blooms in March and April and one flagellate bloom in May together with vertical and horizontal distributions of nutrients, were simulated without tuning of the model to the actual observations. The present simulations support the general idea that flagellates in the coastal areas of the North Sea are stimulated by anthropogenic nutrients, but more specifically that a strong flagellate bloom in the Kattegat-Skagerrak area, corresponding to the *C. polylepis* bloom, was stimulated by such nutrients in May 1988. Although the model should be improved before it is applied in a management context, the great potential of using such models in environmental management is demonstrated.

INTRODUCTION

Mainly because of four reasons, modelling of phytoplankton production is at-

tractive: First, growth is well represented by the equation $dN/dt = \mu N$ where N is number of individuals, t is time and μ is the instantaneous growth rate (in absence of mortality). Although this equation describes a continuous process, while reproduction is discrete, the number of individuals is high and generation time is short and not synchronised, and the assumption about continuity seems adequate. Second, due to binary fission, fecundity is constant. Hence, instantaneous growth rate (μ) depends only on generation time (T_g) according to the relationship $\mu = \ln 2/T_g$. Third, phytoplankton growth potential is generally much higher than the growth potential of their predators. Then, when favourable conditions occur (in terms of light and nutrients), phytoplankton is likely to increase exponentially until the resources are consumed. Fourth, water movements dominate mobility (at least horizontally) rather than individual behaviour. Then, stated somewhat provocative, phytoplankton modelling is essentially a question of correct representation of generation time (or growth rate). At the higher levels of the food-chain the modeller is faced with age classes (N becomes a vector), maturation, variable fecundity including density dependent mechanisms, predators with similar growth potential, mobility dominated by swimming etc. Of course, as in higher trophic levels, phytoplankton growth is also regulated by complex processes at the cellular and biochemical level. Furthermore, phytoplankton consists of an unmanageable number of species (at least to the modeller) having different life history and growth characteristics. Nevertheless, we believe that it is within the area of primary production and nutrient dynamics that ecology is closest to the aim of providing predictive models through integration with physics (physical oceanography and meteorology). The exponential decrease in computing costs is likely to accelerate this development in the near future. Current research on ocean-climate relations and eutrophication also stimulates development of more realistic primary production models.

The present paper emerged during the development of a meteorological, topographical and hydrological driven 3-D baroclinic physical model including state variables of nutrients and phytoplankton biomass of the North Sea, a research activity that is directed against future management. We realised that subjective *a posteriori* tuning of the biological coefficients in order to improve the fit between model predictions and case specific measurements was frustrating and rather unproductive. We wanted objective measures of the predictive power rather than several case-specific tuned versions. This requires several applications of the same model (with the same values of the coefficients) to different data sets. The present paper consists essentially of two parts: The first part reports on the specification and validation of the sink and source terms of a single phytoplankton model. In the second part this module is coupled with a 3-D hydrodynamical model for the North Sea. The spring 1988 is simulated with emphasis on the Skagerrak-Kattegat area. The general productivity of the North Sea as such will be analysed by the model elsewhere (Skogen et al. in press).

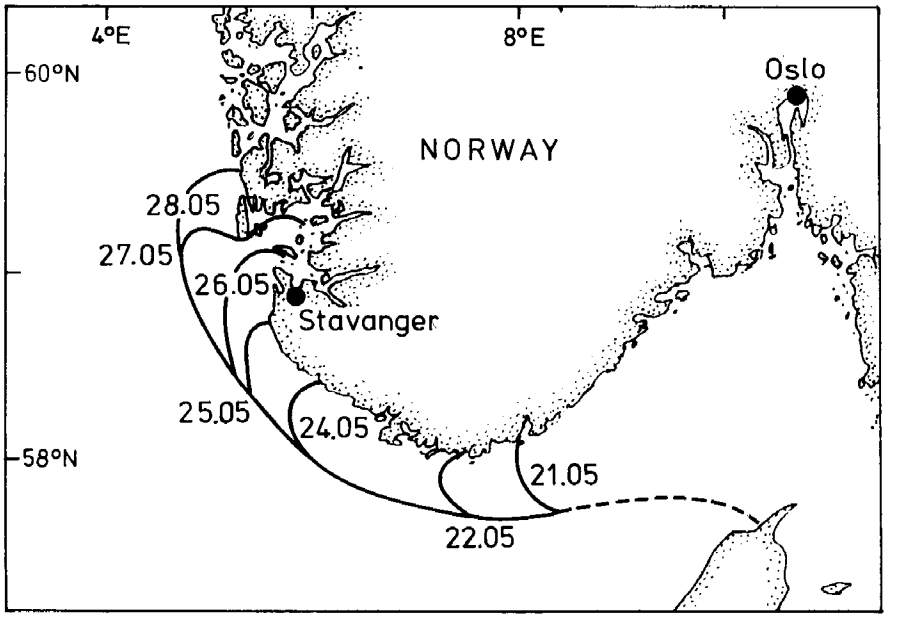

Fig. 1. Spreading of *C. polylepis* along the Norwegian coast during May 1988. Position of the algae "front" is indicated by the dates (modified after Aksnes et al. 1989).

A change in the species composition of phytoplankton in the North Sea and adjacent water has been observed during the last decades. Specifically, it has been a shift from diatom towards flagellate dominance (Nelisson & Stefels 1988, Ziljstra 1988). Furthermore, within the last decade an increasing number of harmful flagellate blooms have been reported in coastal areas of the southern part of the North Sea. This trend culminated in the spring of 1988 with the *Chrysochromulina polylepis* bloom (Aksnes et al. 1989, Maestrini & Granéli 1991, Skjoldal & Dundas 1991). This bloom extended to the western coast of Norway and affected a water body of a size never previously reported (Fig. 1). During a Norwegian cruise, conducted by the Institute of Marine Research in Bergen, high nitrate concentrations were observed west of Denmark and in the deeper waters of the Kattegat-Skagerrak area (Fig. 2 and Fig. 3). Consequently, eutrophication has been focused as causal mechanism, but to what extent this might have contributed to the *C. polylepis* bloom remains unclear (Maestrini & Granéli 1991). The causal mechanisms for such blooms should be sought through experimental work on the algae considered, but also at the temporal and spatial scale of the bloom phenomenon itself. The *C. polylepis* bloom developed on a regional scale of order 10^4-10^5 km^2. Although the North Sea together with the Skagerrak-Kattegat area is one of the most monitored marine waters, no set of time-series' data covered the

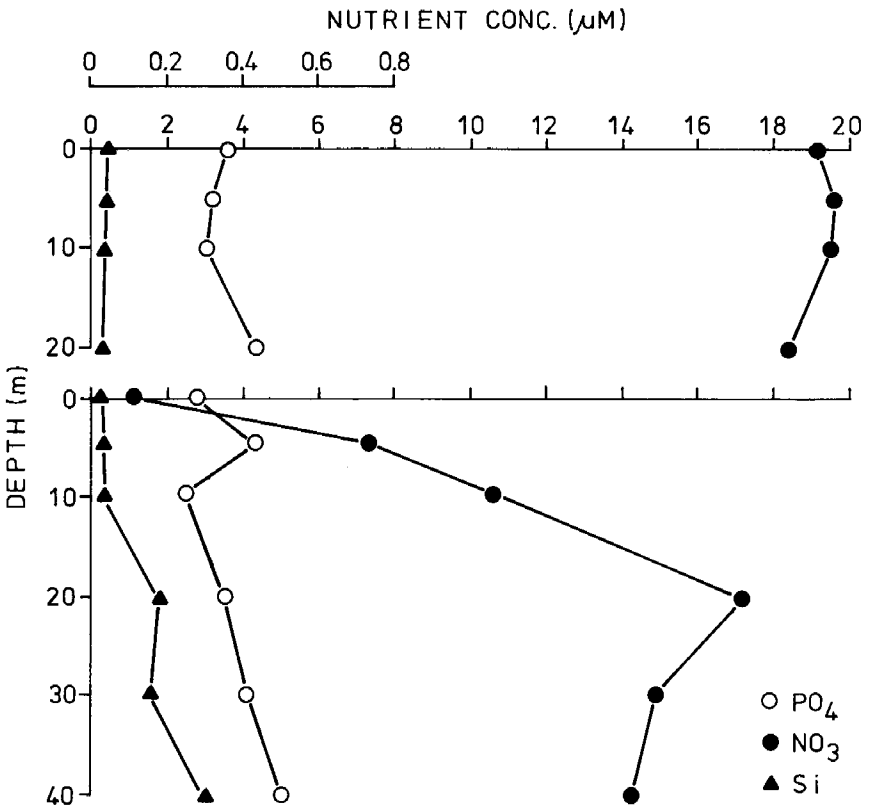

Fig. 2. Vertical profiles of phosphate (upper scale), nitrate and silicate (lower scale) off the west coast of Denmark (upper graph, Station no. 60) and in the northern Kattegat (lower graph, Station no. 109). The measurements were obtained during a cruise with R/V "G. M. Dannevig" in April 1988. (Modified after Skjoldal & Dundas 1991). Position of the two stations are indicated in Fig. 3.

C. polylepis bloom period (Maestrini & Granéli 1991). Also data on the distribution patterns (horizontal and vertical) of central variables such as nutrients, phytoplankton mass and composition are very sparse or missing. We are not arguing that simulation models can substitute such measurements, but they may be extremely helpful for the interpretation and quantification of such phenomenons. In the last part of this paper we present some simulation results of nutrients and phytoplankton dynamics of the North Sea during the spring 1988. Besides the phytoplankton module elaborated in the first part, realistic forcing (i.e. bottom topography, actual meteorology and riverine flow), initialisation data based on measurements and a state-of-the-art hydrodynamical model (Blumberg & Mellor 1987), represent the main element of this approach (Fig. 4). Model formulations and coefficients are selected independently of the actual case that has

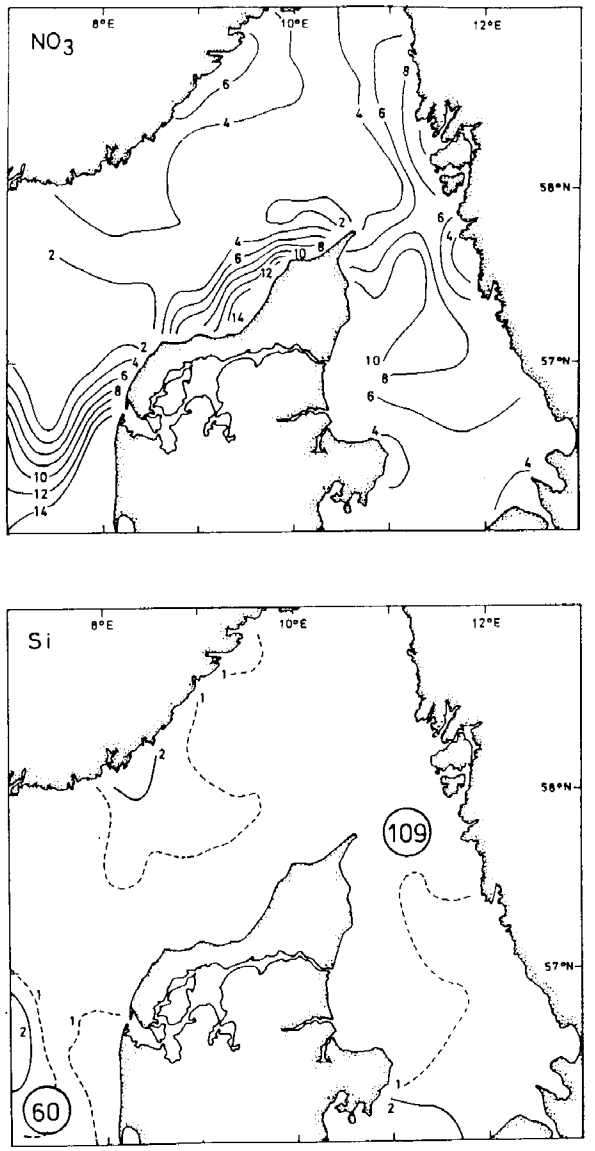

Fig. 3. Average concentrations (μM) of nitrate (upper) and silicate (lower) in the upper 30 m during a cruise with R. V. "G. M. Dannevig" in the period 11-23 April 1988 (taken from Aksnes et al. 1989). The numbers 60 and 109 indicate the position of the two stations referred to in the text.

been simulated. To evaluate the effect of anthropogenic nutrient load on the phytoplankton development, the model was re-run without anthropogenic nutrients.

This work has been supported by the Norwegian Research Council by grants to Dag L. Aksnes, Berit R. Heimdal & E. Svendsen. We would like to thank the Meteorological Institute in Oslo for cooperation and for the preparation of the meteorological hindcast archives, and ICES for provid-

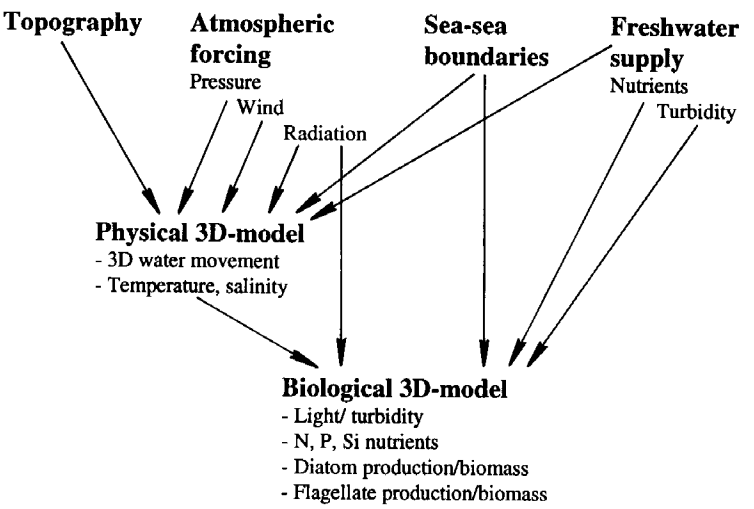

Fig. 4. Main components of a meteorologically driven simulation model for phytoplankton production.

ing initial data on nutrients. Geir Ottersen was most helpful concerning the interpolation of the ICES nutrient data. We thank J. Bartsch for providing us with a climatology for the North Sea. We would also like to thank dr. Jan A. Olseth and Arvid Skartveit for helpful suggestions regarding the modelling of atmospheric light.

SPECIFICATION OF THE PHYTOPLANKTON MODEL

Many numerical ecological models of phytoplankton have been proposed during the last decades. A main problem, however, is to judge the generality and the realism of such models. Usually, model predictions are evaluated against the same date as the model and the values of the process coefficients are based upon, and tuning (or calibrations) of coefficients have been intimately linked to the model formulation. An experienced modeller may easily produce a reasonable fit to observations by adjusting the important coefficients of the model. This is usually justified as such adjustments have been done within reasonable limits (i.e. within actual measurements of the coefficients). With tuning, however, decisive conclusions about the generality and predictability of the model cannot be drawn. Thus, the model can hardly be recommended for a new case (i.e. different forcing such as topography, irradiance, mixing, advection, nutrient input, temperature etc.). As pointed out by Loehle (1983) the process of tuning degrades a more or less "law-based" application model to a "calculation-tool". Although calculation tools may be predictive for specific situations, the domain of applicability is likely to be limited and hard to specify. The present non-tuned phytoplankton model emerged according to the following procedure:

1. Phytoplankton state variables and processes are based upon prevailing representations given in the literature. In this first version we decided to keep the process representation as simple as possible, and to keep the number of state variables low (5) compared to that required by models representing cellular state (such as N:P:C:chlorophyll ratios) internal pools of nutrients, etc.

2. We chose a set of coefficients that has demonstrated good fit to high quality measurements. Presently, we believe that enclosure experiments are providing the most reliable (and relevant) observations on phytoplankton dynamics. Hence, the values of the coefficients are primarily based on those derived by Andersen et al. (1987) and Andersen & Nival (1989) simulating the nutrient and phytoplankton dynamics in the CEPEX-enclosures.

3. We tested the model against three enclosure experiments (with parallels) which were forced differently from the CEPEX enclosures. Calibration was not applied as the purpose of this test was to specify a first objective measure of the predictive ability of the model.

State variables

We feel that the "state-of-the-art" does not allow model resolution at the phytoplankton species level. As pointed out by Andersen et al. (1987), however, one can no longer avoid differentiating between diatoms and flagellates, as these two groups do not have the same physiological characteristics. Such differentiation was successfully used in the simulation models of Kremer & Nixon (1978), Andersen et al. (1987), Andersen & Nival (1989) and Aksnes & Lie (1990). Recent reviews of growth rate characteristics (Furnas 1990) and irradiance relationship (Langdon 1988) in phytoplankton also support a differentiation. The most important reason for a differentiation, however, is the silicate requirement of diatoms. Differentiation into the two groups is also of value in the management context, as toxic species are primarily belonging to the flagellate group. Human eutrophication alters the Si:N:P ratios, and thereby the growth conditions for the two groups (Officer & Ryther 1980, Egge & Aksnes 1992).

The macronutrients, here denoted the N-, P- and Si-nutrients, may all limit phytoplankton growth in coastal waters. Phytoplankton utilise different compounds of the macronutrients such as ammonium and nitrate. Here we consider each nutrient state variable (which are the N, P and Si-nutrients) as representing the sum of all compounds (that can be utilised by phytoplankton) of the macro-element under consideration. An alternative is to represent the different compounds as different state variables. Then phytoplankton growth dynamics has to be specified for each compound as well as the chemical transitions between the compounds. Presently, this is hardly recommended as this implies an incredible increase in the number of rather uncertain coefficients. The aggrega-

tion of related nutrient compounds into a common state variable is of course introducing bias in the uptake specification which is based primarily on one compound (such as nitrate). The errors associated with the aggregation of nutrient compounds and phytoplankton species are not necessarily serious and can only be assessed through applications.

Maximum phytoplankton growth rates

For models running over a seasonal cycle, specification of growth rate versus temperature is crucial. Both the level of maximum growth rate and its temperature dependency have to specified. For a single species, growth rate is likely to have a temperature optimum. In a group representing several species (such as diatoms), however, the different species have different temperature optimums. Then, maximum growth for the group increases with temperature according to a specific shift along with the temperature increase. This increase is primarily reflecting a general speed-up in the biochemical machinery of the cells. The Q_{10}-concept is commonly used to express the temperature influence on biochemical reactions. A $Q_{10} = 2$ means that the rate of a reaction increases with a factor of two when temperature is increased 10°C. The relationship may be expressed:

$$\mu_{max}(T) = \mu_{max0}\, e^{a_1 T} \qquad (1)$$

where μ_{max} (T) is maximum growth rate at temperature T, μ_{max0} is maximum growth rate at 0°C and $a_1 = \ln Q_{10}/10$. Thus it is assumed that maximum growth is exponentially related to temperature. Of course, the above expression is not valid at high temperatures, as Eq. 1 predict growth to increase infinitely with temperature. For the interval 0-25°C, however, it should be considered as a good description. Thus, for most marine applications Eq. (1) seems valid. The review of Eppley (1972) indicates a Q_{10} for phytoplankton growth of 1.88, corresponding to an $a_1 = 0.063$.

Andersen & Nival (1989) arrived at a maximum growth rate of diatoms of 3 d^{-1} at 13°C. Assuming this value and $a_1 = 0.063$, we obtain by the use of Eq. (1): $\mu_{d.max0} = 1.5\ 10^{-5}\ s^{-1}$ for diatoms (Table 1). The review of Furnas (1990) clearly indicates that the flagellates as a group has a lower growth rate than diatoms. Furthermore, modelling the CEPEX experiments, Andersen & Nival (1989) found good fit to observations by assuming that the maximum microflagellate growth rate was 2/3 of the maximum diatom growth rate. Hence, we arrive at a $\mu_{f.max0} = 1.0\ 10^{-5}\ s^{-1}$ for flagellates. We have not found strong evidence for the use of different Q_{10}'s for diatoms and flagellates, although this has been applied by Kremer & Nixon (1978), Andersen & Nival (1989) and Aksnes & Lie (1990). Hence, we suggest use of the same a_1-value for the two phytoplankton groups (Table 1).

Table 1. State variables and values of the coefficients of the phytoplankton model. A reference is given to the equation where the coefficients appear.

Symbol	Value/unit	Explanation
Maximal growth versus temperature (Eq. 1)		
$\mu_{d.max0}$	$1.5\ 10^{-5}\ s^{-1}$	Maximum growth rate for diatoms at 0°C
$\mu_{f.max0}$	$1.0\ 10^{-5} s^{-1}$	Maximum growth rate for flagellates at 0°C
a_1	$0.063\ °C^{-1}$	Temperature dependency of growth, diatoms and flagellates
Growth limitations (Eq. 4 and 5)		
$\alpha_{d.N}$	$1.7\ 10^{-5}\ s^{-1}\mu M^{-1}$	Diatom affinity for nitrogen-nutrients
$\alpha_{d.P}$	$2.7\ 10^{-4}\ s^{-1}\mu M^{-1}$	Diatom affinity for phosphorus-nutrients
$\alpha_{d.Si}$	$2.5\ 10^{-5}\ s^{-1}\mu M^{-1}$	Diatom affinity for silicon-nutrients
$\alpha_{d.I}$	$3.6\ 10^{-7}\ m^2\mu E^{-1}$	Diatom affinity for light
$\alpha_{f.N}$	$1.5\ 10^{-5}\ s^{-1}\mu M^{-1}$	Flagellate affinity for nitrogen-nutrients
$\alpha_{f.P}$	$2.3\ 10^{-4}\ s^{-1}\mu M^{-1}$	Flagellate affinity for phosphorus-nutrients
$\alpha_{f.I}$	$1.1\ 10^{-7}\ m^2\mu E^{-1}$	Flagellate affinity for light
Mortality (Eq. 6)		
m_d	$1.6\ 10^{-6}\ s^{-1}$	Diatom mortality rate
m_f	$1.6\ 10^{-6}\ s^{-1}$	Flagellate mortality rate
Metabolic losses (Eq. 7)		
e_0	$8.1\ 10^{-7} s^{-1}$	Metabolic loss rate at 0°C, diatoms and flagellates
a_2	$0.07\ °C^{-1}$	Temperature dependency of metabolic losses, diatoms and flagellates
Diatom sinking rate (Eq. 8)		
Si_t	1.0 μM Si	Threshold silicate concentration
w_{max}	$3\ m\ d^{-1}$	Maximum sinking rate
w_{min}	$0.3\ m\ d^{-1}$	Minimum sinking rate
a_3	$2.7\ \mu M\ m\ d^{-1}$	Shape factor for the sinking function
Cellular elemental composition (mol-ratio)		
r_1	.0625	P:N ratio in diatoms
r_2	.0625	P:N ratio in flagellates
r_3	.875	Si:N ratio in diatoms

Environmental Limitations – from maximum growth rate to realised growth rate

The temperature specific maximum growth rate is seldom realised under natural conditions. The complex biochemical reactions involved in growth may be limited by several different chemical compounds (both organic and inorganic) and energy. As outlined above, we consider only the most important (at least the most well-known) limitations, i.e. the N, P, Si and light limitations. The Monod expression (or Michaelis-Menten when considering nutrient uptake instead of growth):

$$\mu' = \mu_{max} S/(K_s + S) \quad (2)$$

has been widely used in experimental work and consequently in simulation models. Here, μ' is the realised growth rate when only S is limiting, μ_{max} is the temperature specific maximum (given by Eq. 1), S is the ambient nutrient concentration (or irradiance) and K_s is the "half saturation constant". Both experimental and theoretical evidence support the use of the non-dimensional limitation term $S/(K_s + S)$. K_s, however, can hardly be regarded as a constant in an environmental context (Aksnes & Egge 1991). In fact K_s should (by definition) depend on temperature in the same way as growth rate (μ_{max}) unless the affinity (see below) is highly temperature variable. A constant K_s, has, at least to our knowledge, been universally applied in simulation models. Although this may be adequate for many applications (especially when temperature can be considered constant), we feel that the constant half-saturation concept should be abandoned in models where temperature is allowed to vary (at the interval 0-25°C in the present application). Following Aksnes & Egge (1991), we suggest the use of a constant "growth affinity" coefficient instead:

$$\mu' = \mu_{max} S/(\mu_{max}/\alpha_s + S) \quad (3)$$

Thus, values of the affinities (α_s) rather than half saturation's have to be specified. This is trivial, however, as $\alpha_s = \mu_{max}/K_s$. At first sight it may look peculiar that the substitution of K_s ($= \mu_{max}/\alpha_s$) alters anything at all. What is really achieved, however, is that the use of a constant affinity implies the use of variable half saturation (as μ_{max} varies with temperature). This may give a quite dramatic effect on the calculated growth rate at low nutrient concentrations. The affinity associated with growth (α_s) may also be temperature dependent, but presumably to a much lesser extent than K_s (Aksnes & Egge 1991).

Eq. (3) expresses the realised growth rate when only one environmental factor (S) is limiting. The "law of the minimum" is commonly applied when several nutrients are limiting simultaneously, i.e. the factor being most limiting is taken into account while the others are not. Simultaneous light and nutrient limitation, however, is commonly represented, as in the model of Andersen & Nival (1989), by multiplicative limitation. (i.e. the realised limitation is the product of each limitation term). Accordingly, we include the following algorithm for calculation of the realised growth rate of diatoms (μ_d):

$$\mu_d = \mu_{d.max} (I/ (\mu_{d.max}/\alpha_{d.I} + I)) S_{d.lim} \quad (4)$$

$$S_{d.lim} = MIN(N/(\mu_{d.max}/\alpha_{d.N} + N), P/(\mu_{d.max}/\alpha_{d.P} + P), Si/(\mu_{d.max}/\alpha_{d.Si} + Si))$$

where I, N, P and Si are ambient photosynthetic active radiation (PAR), nitro-

gen-, phosphorus- and silicon-nutrient concentrations respectively, and $\alpha_{d.I}$, $\alpha_{d.N}$, $\alpha_{d.P}$, $\alpha_{d.Si}$ are the diatom growth affinities for PAR, nitrogen, phosphorus and silicon nutrients. Correspondingly, for the flagellates:

$$\mu_f = \mu_{f.max} (I/ (\mu_{f.max} /\alpha_{f.I} + I)) S_{f.lim} \quad (5)$$

$$S_{f.lim} = MIN(N/(\mu_{f.max}/\alpha_{f.N} + N), P/(\mu_{f.max}/\alpha_{f.P} + P))$$

as our flagellate group is not limited by silicon.

We have not included the effect from photoinhibition, and this means that the model may give biased growth at high irradiance. The reason for avoiding photoinhibition is that this inevitably brings up the question of also representing photoadaptation. Reasonable values for such representations may be obtained for single species studied under laboratory conditions, but is more hard to derive for aggregated groups of phytoplankton species.

For diatoms Andersen and Nival (1989) used a maximum growth rate of 3 d^{-1}, and half saturation's for nitrate and silicate of 2.0 and 1.4 μM respectively. These values correspond to the affinities: $\alpha_{d.N} = 1.7\ 10^{-5}$ and $\alpha_{d.Si} = 2.5\ 10^{-5}\ s^{-1}\ \mu M^{-1}$. Andersen & Nival (1989) did not include phosphorus dynamics. The Redfield ratio serves as a good approximation for the cellular N:P ratio (16:1) in aggregated phytoplankton groups. Although the cellular N:P ratio is known to vary, representation of N:P dynamics at the cellular level requires at least one additional state variable (cellular phosphorus content) and several additional coefficients. Therefore, we assume a constant N:P ratio (16:1) and that growth affinity is 16 times higher for the P-nutrients than for the N-nutrients ($\alpha_{d.P} = 2.7\ 10^{-4}\ s^{-1}\mu M^{-1}$). Furthermore, a constant Si:N ratio is assumed.for the diatoms.

Langdon (1988, Table IX) reports light affinities (with respect to growth rate) for several groups of phytoplankton on the range $0.51\ 10^{-3}$ - $63\ 10^{-3}$ div. $day^{-1}\mu E^{-1}\ m^2$ s which, in our units, corresponds to α_I on the range $4.3\ 10^{-9}$ - $5.1\ 10^{-7}\ m^2\ \mu E^{-1}$. One of his main conclusion was that the diatoms, as a group, were best adapted to grow at low light (i.e. high growth affinity for light). Andersen et al. (1987) and Andersen & Nival (1989) used the growth - irradiance relationship by Peters & Eilers (1978) where neither half saturation nor affinities are explicitly parameterized. Nevertheless, we approximated the affinity-value on the basis of their representation and arrived at $\alpha_{d.I} = 3.6\ 10^{-7}\ m^2\ \mu E^{-1}$ which is in the upper range of the values reported by Langdon (1988). For flagellates Andersen and Nival (1989) used a maximum growth rate of 2 d^{-1}, and a half saturation for nitrate of 1.5 μM respectively. These values give the growth affinity $\alpha_{f.N} = 1.5\ 10^{-5}\ s^{-1}\ \mu M^{-1}$. Here, we also assume that the growth affinity is 16 times higher for P-nutrients than for N-nutrients ($\alpha_{f.P} = 2.3\ 10^{-4}\ s^{-1}\ \mu M^{-1}$). The growth affinity for light was approximated on the basis of the growth-light representation for the microflagel-

late group of Andersen & Nival (1989): $\alpha_{f,I} = 1.1\ 10^{-7}\ m^2\mu E^{-1}$, which is lesser than the diatom value, but still in the upper range of the values reported by Langdon (1988).

Losses

We have included three phytoplankton loss terms; mortality, metabolic losses and diatom sinking. The mortality formulation of Andersen & Nival (1989) includes four coefficients for each phytoplankton group as mortality is assumed to depend nonlinearly on nutrient concentration. We have simplified this representation and assume a constant instantaneous mortality rate for both flagellates (m_f) and diatoms (m_d). The mean of Andersen & Nival's (1989) m_m-values (0.1 and 0.18 d^{-1}, see their Table 4.) was chosen for both groups:

$$m_f = m_d = 1.6\ 10^{-6}\ s^{-1} \tag{6}$$

In nature, mortality is reducing the population number (and hence the total biomass), while metabolic losses (excretion) is only reducing the biomass. In models representing biomass rather than numbers the two losses may seem identical. The loss according to mortality, however, is not readily available for regenerated production (it is commonly put into a detritus-variable or grazer), while the metabolic losses are commonly added to the nutrient state variables and become immediately available for uptake by the phytoplankton (regenerated production). As Aksnes & Lie (1990) we assume that the instantaneous metabolic loss rate is the same for both groups (e_f and e_d) and depends on temperature (T) according to:

$$e_f = e_d = e_0\, e^{a_2 T} \tag{7}$$

where e_0 is the metabolic loss at 0°C, and a_2 represents the temperature dependency of the process ($\ln Q_{10}/10$).

Sinking of diatoms (w_d) depends on the silicate concentration according to Andersen & Nival (1989):

$$\text{If } Si \leq Si_t \text{ then } w_d = w_{max} \tag{8}$$

$$\text{If } Si > Si_t \text{ then } w_d = (a_3/Si + w_{min})$$

where w_{min}, w_{max}, Si_t and a_3 are minimal and maximal sinking rate, threshold silicate concentration and shape factor for the curve sinking rate versus silicate concentration respectively (Because of the continuously stirring, sinking was not applied in the validation experiment presented in the next section).

Zooplankton grazing is an obvious loss term not explicitly accounted for in the present model (although a mortality term is included). Dynamic representation of grazing requires dynamic representation of the herbivore standing stock, which again requires a representation of the mortality acting on this stock and so on. Presently we feel that it is desirable to "close" the model at the phytoplankton level as representations of the higher levels introduce intractable problems (see Introduction). Hence, the model will behave badly if phytoplankton under grazing control is to be simulated (i.e. in situations where the phytoplankton is not able to utilise nutrients due to extreme grazing pressure).

A VALIDATION EXPERIMENT OF THE PHYTOPLANKTON MODULE

Results from enclosure experiments conducted in Raunefjorden (close to Bergen at the western coast of Norway) were used as validation data. Methodological details of these and similar experiments have been given by Egge & Aksnes (1992) and Bratbak et al. (1993) and only a short description is given below. Six enclosures (4 m deep and with a volume of 11 m^3) were attached to a floating laboratory in the period June 13 - July 11, 1990. Two bags (parallels) were added nitrate, inorganic orthophosphate and silicate (denoted NPS-experiments), two were added nitrate and inorganic orthophosphate (NP-experiments, to provoke silicon limitation), and another two nitrate and silicate (NS-experiment, to provoke phosphorus limitation). Water was pumped continuously (40 l min^{-1}) from the bottom to the top of the enclosure in order to ensure a homogenous distribution of nutrients and phytoplankton. Each bag was renewed with natural water from the outside of the bags at a rate of 10% per day. Samples for nutrients, phytoplankton enumeration and identification (together with several other environmental parameters not reported here) were taken daily in the enclosures as well as in the incoming water (boundary conditions to the model). In calculation of C-values (Eq. 11), cell counts were converted into N-biomass (flagellates and diatoms) according to size measurements of the dominating species. This approximation of "observed" phytoplankton biomass, however, is rather biased and does not allow detailed comparisons between model output and observations of the time development in the two phytoplankton groups. Hence, the nutrient rather than phytoplankton dynamics is focused in the comparison of model output with data.

Simulation model

Each state variable was represented by a differential equation (Table 2). Initial values of the state variables were measured, and the forcing of the model included

Table 2. The simulation model of the enclosure experiments. The coefficient k_1 (=1.16 10^{-6} s^{-1}) represents the 10% per day water renewal of the enclosures while N_b and N_{add} represent the nitrogen nutrient concentration in the incoming water and the added nitrogen fertiliser respectively. μ_d and μ_f are the diatom and flagellate growth rate given by Eq. (4) and (5) respectively, while e_d and e_f are the diatom and flagellate metabolic loss rate given by Eq. (7). The values of r_1, r_2, r_3, m_d and m_f are given in Table 1.

Nitrogen nutrients (N):
$$dN/dt = -k_1 (N-N_b)+N_{add}-D(\mu_d-e_d)-F(\mu_f-e_f)$$

Phosphorus nutrients (P):
$$dP/dt = -k_1 (P-P_b)+P_{add}-r_1D(\mu_d-e_d)-r_2F(\mu_f-e_f)$$

Silicon nutrients (Si):
$$dSi/dt = -k_1 (Si-Si_b)+Si_{add}-r_3D(\mu_d-e_d)$$

Diatoms (D):
$$dD/dt = -k_1 (D-D_b)+D(\mu_d-e_d-m_d)$$

Flagellates (F):
$$dF/dt = -k_1 (F-F_b)+F(\mu_f-e_f-m_f)$$

measurements of surface irradiance, water temperature, nutrient addition, and measurements of the state variables in the incoming water (boundary conditions). As the water of the bags was mixed continuously, we assumed that all phytoplankton experienced the same average light regime. Ideally, for the present validation purpose the mean light within the enclosures should have been measured continuously and used to force the model. Instead the mean irradiance of the enclosures was calculated on the basis of above surface measurements of hourly incident irradiance at the Radiation observatory, University of Bergen (Anon. 1991). The subsurface irradiance had to be calculated on the basis of these measurements. Solar elevation and self-shading from phytoplankton biomass was also taken into account in this calculation. The diffuse light (I_{dif}) and direct (I_{dir}) light at depth z was calculated as:

$$\begin{aligned} I_{dif}(z,t) &= b_1 R_{dif}(t) e^{-K_{dif} Z} \\ I_{dir}(z,t) &= b_1 R_{dir}(t) e^{-K_{dir} Z} \end{aligned} \qquad (9)$$

where $R_{dif}(t)$ and $R_{dir}(t)$ are the diffuse and direct components of the surface irradiance which are converted into PAR by the constant b_1 . K_{dif} and K_{dir} are the diffuse and direct attenuations of the water column given by:

$$\begin{aligned} K_{dif} &= (b_2 + b_3 + b_4(D+F))/\zeta \\ K_{dir} &= (b_2 + b_3 + b_4(D+F))/(\cos\theta) \end{aligned} \qquad (10)$$

where the coefficients represent attenuation due to sea water (b_2), attenuation due to dead particulate matter and dissolved compounds (b_3), attenuation due to diatoms (D) and flagellates (F), ζ represents the mean path length per unit vertical distance in the water column for the diffuse light rays and is equal to 0.83 (Sathyendranath & Platt 1990), and finally θ is the zenith angle of the direct light in the water column computed from Snells formula.

As Jørgensen et al. (1986) and Andersen & Nival (1989) we calculated the general standard deviation defined as:

$$C = \left(\sum_{i=1}^{n} (x_t - x_m)^2\right)^{1/2} / n x_m \qquad (11)$$

where x_t is the predicted value of the model, x_m the measured data, x_m is the mean of x_m and n the number of pairs of figures compared.

Model prediction versus measurements

NPS-experiment. The predicted nitrogen nutrients and nitrate-measurements are fairly coincident (C = 0.16, Fig. 5). The P-nutrients predicted by the model was consistently higher than the phosphate-measurements (C = 0.21), however, indicating a too low cellular P:N-ratio in the model. The silicate levels drop off more rapidly than predicted by the model (C = 0.19), but the selected N:Si ratio seems realistic as both measurements and model predictions indicate silicate limitation at the end of the experimental period. Integrated for the entire period, the model predicted that diatoms corresponded to 64% of the N-biomass (36% flagellates). The observations indicated that 73 and 74% of the cell numbers were diatoms in the two parallel enclosures. The C-values were 0.32 and 0.29 for diatoms and flagellates respectively. As stated earlier, however, these values are affected by the error associated with conversion from cell number to N-biomass.

NP-experiment. Also here the simulated N-nutrients and the observed nitrate concentrations corresponded well (C = 0.08, Fig. 6). Again, the simulated P-nutrients were consistently higher than the phosphate measurements (C = 0.23). These enclosures were not silicate enriched, and low silicate values were both measured and modelled (C = 0.36). Integrated for the entire period, the model predicted that diatoms corresponded to 23% of the N-biomass, while the observations indicated that 45 and 55% of the cells were diatoms in the two parallel enclosures. The C-values were 0.31 and 0.42 for diatoms and flagellates respectively.

NS-experiment. Due to the phosphorus limitation, the nitrate concentrations decreased far more slowly than in the NPS and NP experiments (C = 0.04, Fig. 7).

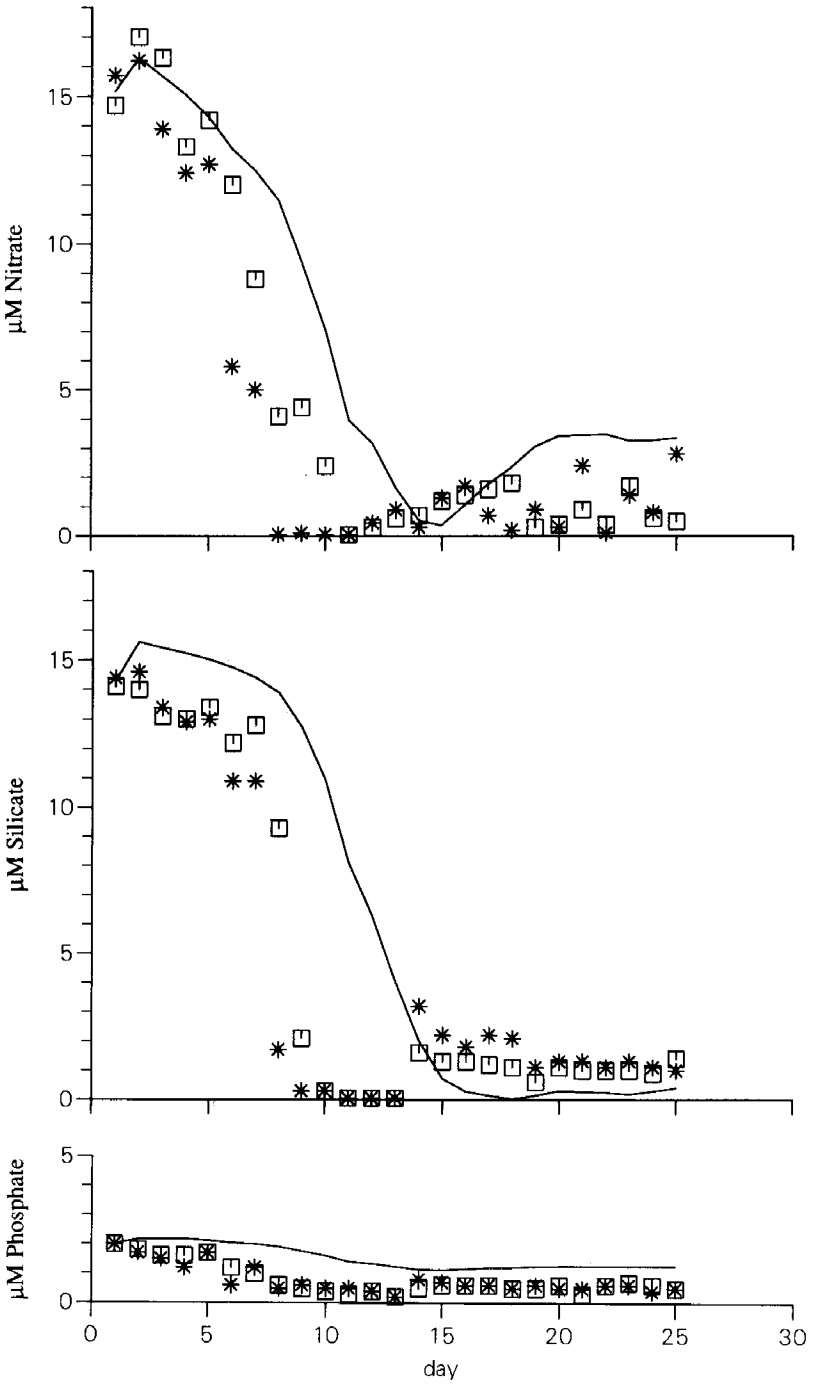
µM Nitrate
µM Silicate
µM Phosphate
0
5
10
15
20
25
30
day

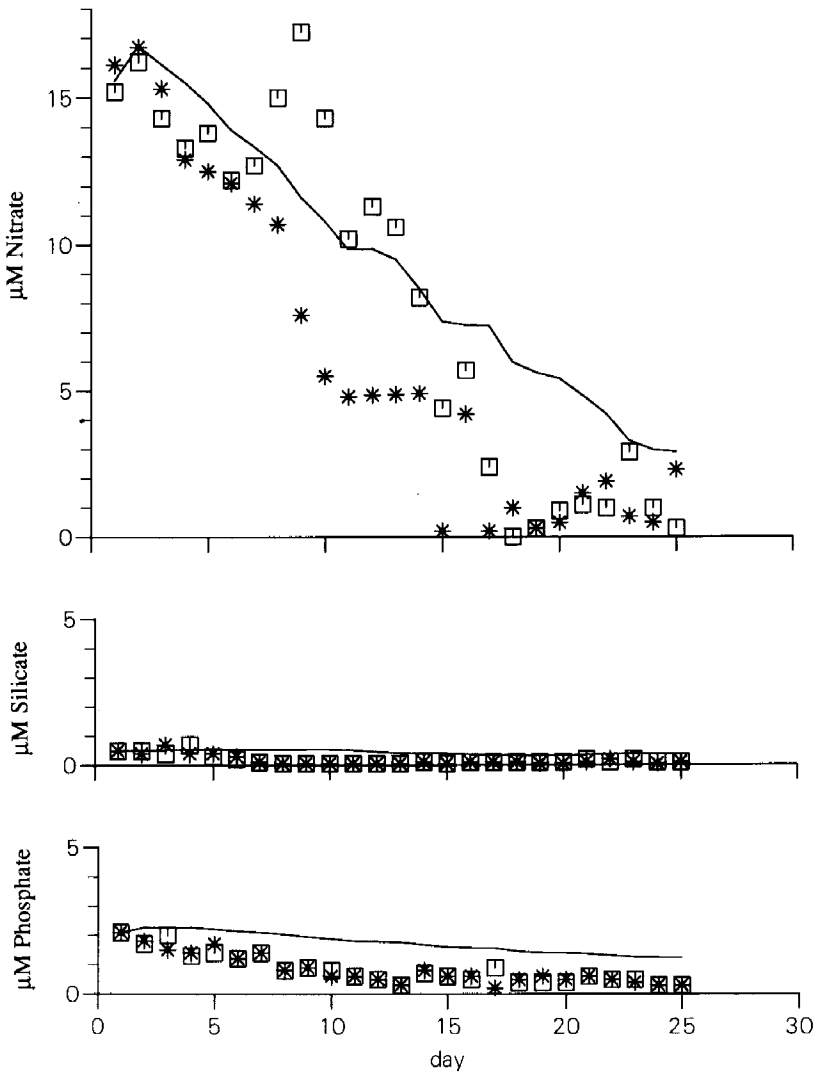

Fig. 6. Mesocosm NP-validation experiment (addition of nitrate and inorganic orthophosphate). Symbols (two parallel experiments) and lines indicate measurements and model predictions respectively.

Fig. 5. Mesocosm NPS-validation experiment (addition of nitrate, silicate and inorganic orthophosphate). Symbols (two parallel experiments) and lines indicate measurements and model predictions respectively.

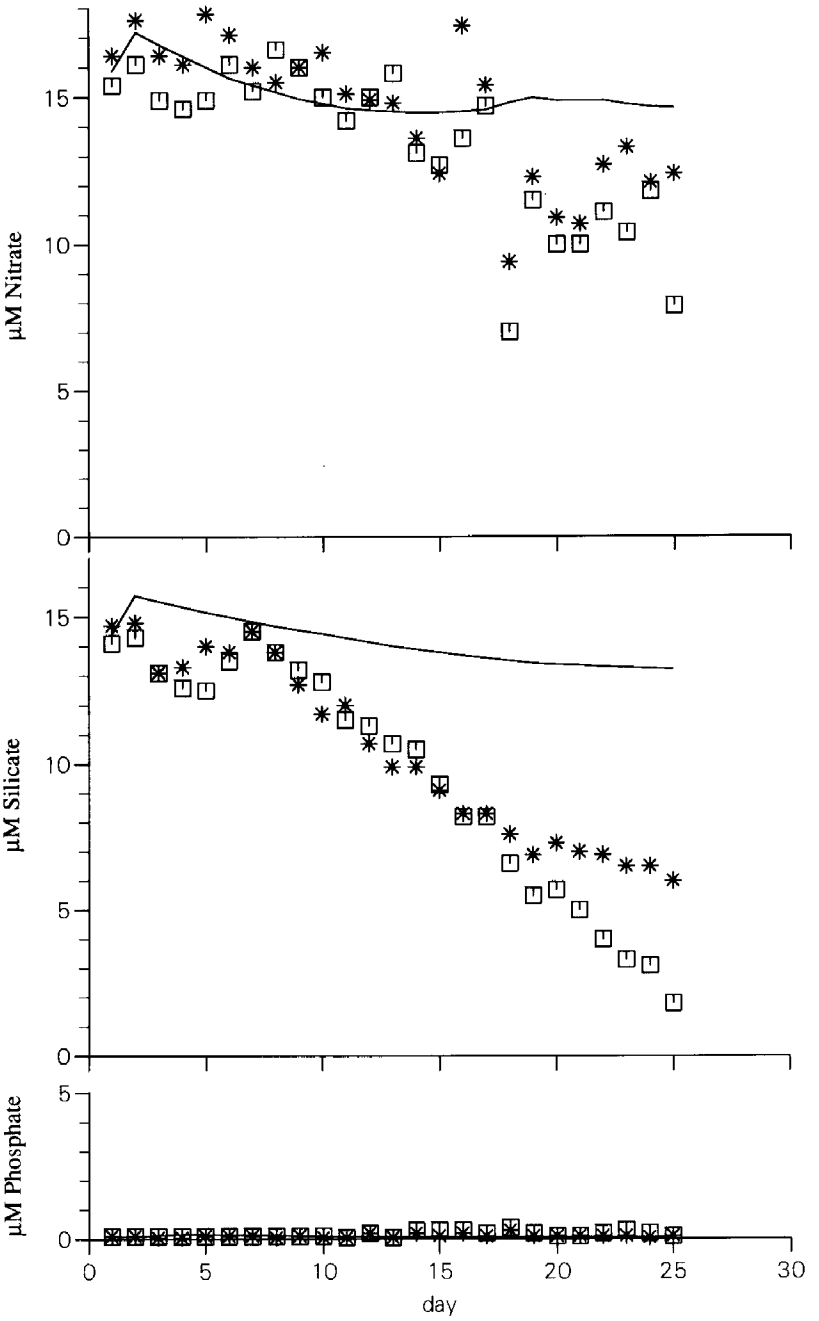

Fig. 7. Mesocosm NS-validation experiment (addition of nitrate and silicate). Symbols (two parallel experiments) and lines indicate measurements and model predictions respectively.

The simulated N-nutrients coincided well with the scattered observations the first two weeks. During the last period, however, more nitrate seems to be utilised in the enclosures than in the model. The same pattern, but even more pronounced, is seen in the silicate development. In contrast to the NPS- and NP-experiments, the simulated P-nutrients were not consistently higher, but rather lower (at least during the last period), than the phosphate measurements (C = 0.15). Integrated for the entire period, the model predicted that 1% of the N-biomass were diatoms, while the observations indicated that 6 and 7% of the cells were diatoms in the two parallel enclosures. The C-values were 0.25 and 0.13 for diatoms and flagellates respectively.

The fit between model predictions and observations can hardly be characterised as impressive, and better correspondence between models and data has been demonstrated elsewhere. As such, in calibrated simulations, Andersen & Nival (1989) obtained C-values of .031 (ours: 0.04-0.16) and 0.069 (ours: 0.10-0.36) for nitrate and silicate respectively and values on the range 0.187-0.325 (ours: 0.13-0.42) for the phytoplankton groups. Nevertheless, the model demonstrates some predictive capability, and a meteorologist would probably be happy with a model providing similar correspondence between prognosis and real weather conditions. A main feature reflected by the model is the strong influence of silicate on the diatom/flagellate composition causing diatom dominance at high silicate concentrations (see also Aksnes & Egge 1991). For management purposes, this may be an important feature as the diatom/flagellate ratio is of considerable interest in the eutrophication debate. Both with respect to the probability of toxic flagellate blooms and for possible food-chain effects.

When comparing our approach with several other approaches in ecological modelling two aspects should be taken into consideration: Firstly, the model formulations and the values of the coefficients were selected entirely independent from the experimental data themselves. Secondly, the validation test must be considered rather strong because the validation experiments provoked, for some periods, all four limitations in the model: light-, nitrogen-, phosphorus- and silicon-limitation (i.e. the non-dimensional limitation terms in Eqs. 4 and 5 were far below 1 at several occasions). Light was the most limiting factor (mainly because the daily light cycle includes dark nights) during the initial phase of the NPS-experiment (high concentrations of nitrate, silicate and phosphate). Thus, the light limitation of the model seems realistic as the decrease in N-nutrients was reflected by the model. In the NP-experiment both light and silicate were limiting for phytoplankton growth. This is reflected in the slower rate of decrease in the nitrate concentrations in the NP-experiment (Fig. 6) compared to the NPS-experiment (Fig. 5). This feature is also reflected by the model, although to a less extent. In the phosphorus-limited NS-experiment, the nitrate utilisation was much slower than in the NPS- and NP-experiments, a feature clearly reflected by the model (Fig. 7).

An obvious bias in the P-dynamics is the ignorance of dissolved organic phosphorus as a nutrient source. An additional nutrient state-variable representing DOP may increase the realism of the model (in cases when phosphorus is limiting). Di Toro et al. (1977) did this and assumed a conversion from organic-phosphorus to orthophosphate at a rate of 3% per day at 20°C. In the North Sea application presented in the next section a state variable representing organic nitrogen/phosphorus is included.

SIMULATION OF NUTRIENTS AND PHYTOPLANKTON DISTRIBUTION OF THE NORTH SEA SPRING 1988

The physical model

The modelled area is characterised by the bottom topography and the land contours (Fig. 8). The physical circulation and dispersion model is a three-dimensional baroclinic model (Blumberg & Mellor 1987). The dependent variables are temperature, salinity, horizontal and vertical water movements and two parameters defining the turbulence by a functional relationship. These two parameters are the turbulent kinetic energy and the length scale of the turbulent eddies. The nutrient and phytoplankton state variables are influenced by water movements and turbulence in the same way as temperature and salinity (see Fig. 9).

The forcing of the physical model is represented by the wind, the atmospheric pressure and riverine fluxes (Fig. 4). The wind regime and the atmospheric pressure for the time period of interest are obtained from the hindcast archives available at the Norwegian Meteorological Institute. Precipitation/evaporation is not included in the physical model. Instead, the salinity and the temperature in the surface waters are relaxed towards climatological fields for the temperature and the salinity in the ocean surface. Except from the Baltic, the FRS (Flow Relaxation Scheme) is implemented at the open boundaries as described by Martinsen & Engedahl (1987). The flow from the Baltic is implemented after an algorithm due to A. Stigebrandt (Gothenburg University, Sweden). Using a horizontal grid size of 20 km all inflow is placed at Storebelt. The flow through Storebelt is determined from the difference in water level between Kattegat and the Baltic. The water entering the Kattegat from the Baltic is characterised by a salinity of 8.0 in the model. The climatological boundary and initialisation fields of temperature, salinity and velocities are modified from fields obtained from J. Bartch (Institut für Meereskunde, Germany) and coupled to temperature and salinity fields outside the North Sea from Levitus (1982). River runoff is parameterized by the flow and the concentrations of macronutrients (see below).

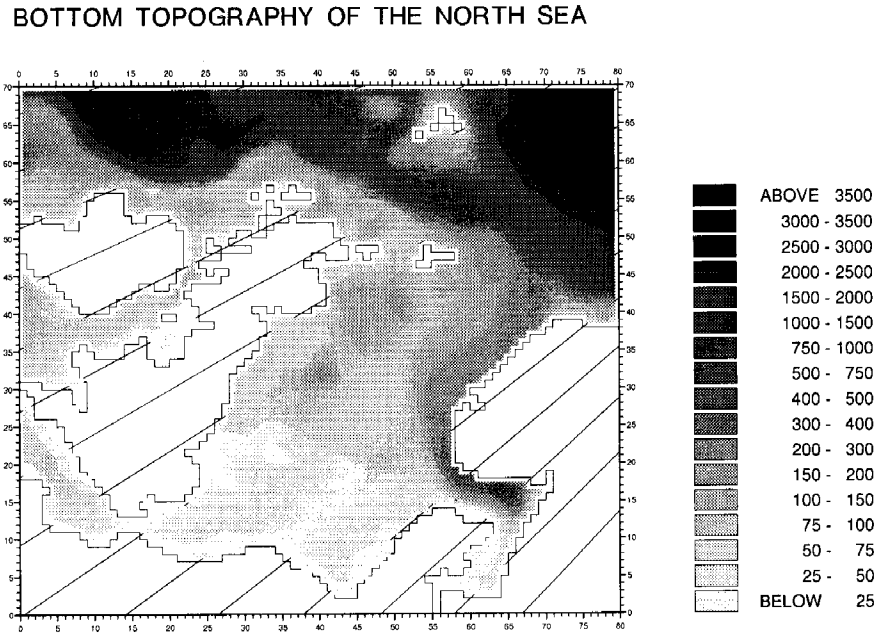

Fig. 8. The modelled area with bottom topography (scale in meters) and land contours. The horizontal grid size is 20 km.

To advance the numerical approximations of the prognostic variables in time a mode splitting technique is applied. In the external mode computations the water level and vertically integrated velocities are updated. Due to stability constraints the time step of the external mode (2-dimensional) computations must be much smaller than the time step of the internal mode computations. In the inter-

General equation for local change in biomass (D):

$$\frac{\delta D}{\delta t} + (w+w_d)\frac{\delta D}{\delta z} + u\frac{\delta D}{\delta x} + v\frac{\delta D}{\delta y} = \frac{\delta}{\delta z}(K_z\frac{\delta D}{\delta z}) + \frac{\delta}{\delta x}(K_x\frac{\delta D}{\delta x}) + \frac{\delta}{\delta y}(K_y\frac{\delta D}{\delta y}) + (\mu\text{-m-e})D$$

Sinking and water transport	Turbulent water movements	"Biology"

Fig. 9. The equation for state change in chemical and biological variables exemplified by the equation for diatom biomass (D) including water transport, turbulent water movements, sinking (w_d, diatom specific) and the biological source (μ; growth) and sink (e; metabolic loss and m; mortality) terms t, z, x and y represent time, the vertical dimension and the two horizontal dimensions respectively, u, v and w the advective parameters and finally K_z, K_x and K_y the turbulent parameters.

nal mode steps all 3-dimensional prognostic variables are updated.

The physical state variables are solved numerically by the leap frog method on a finite difference Arakawa C-grid. Because of the requirement of having positive definite field variables in the chemical and biological state variables, the differential equations for these variables are integrated by use of the upstream method. This integrating scheme is rather diffusive and is therefore used in conjunction with a flux-correcting method (Lehman 1988). In the vertical a sigma coordinate representation is used. In this representation the sea surface is mapped to 0 and the bottom to - 1. The number of layers are 11. At 100 m depth the layers are 0.5 m, 0.7 m, 1.3 m, 2.5 m, 5 m, 10 m, 20 m, 20 m, 20 m, 15 m and 5 m thick and 10 times these values at 1000 m bottom depth. The horizontal grid dimension is 20 kilometres.

Unfortunately, irradiance data does not have the same geographical coverage as other meteorological data, and we based our light representation on daily totals of global radiation from the weather station Taastrup in Denmark (provided by the World radiation data centre, Anon. 1989) and a model of incident surface irradiance by Skartveit and Olseth (1986). The light in the water column was calculated according to Eqs. 9 and 10.

Nutrient load and initial data of nutrients and phytoplankton

As described in a previous section the macronutrients are represented by the elements nitrogen, phosphorus and silicon where nitrate, phosphate and silicate are considered as the main components respectively. Data from Februar 1988 are obtained from ICES (Copenhagen, Denmark) and used for initialisation. The data coverage is horizontally relatively dense in the surface areas of the central parts of the North Sea, the Kattegat and the Skagerrak. Measured data are not provided for in the English Channel, the northern parts of the North Sea, the Irish Sea and the oceanic areas west of Ireland. In these areas we have used typical data from a winter situation as given in Ziljstra (1988). In the vertical direction, the data coverage is more sparse. Often there are only two measurements in the water column. In February, however, the water column and the nutrients are well mixed.

Since the model requires values in every grid cell, the data are interpolated using a procedure by Ottersen (1991). This interpolation procedure used a combined cubic spline laplacian interpolation method. Input of nutrients from 23 rivers in 6 countries are included. These are: 1) Norway: Glomma. 2) Sweden: Ätran, Bäveån, Enningdalsälven, Göta-älv, Lagan, Nissan, Örekils älven, Rönne å and Viskan. 3) Germany: Elbe, Ems and Weser. 4) Holland: The Rhine at Haringvliet, Noordzeekanaal, Massluis Lake Ijssel. 5) Belgium: Scheldt. 6) England: Forth, Humber, Tees, Thames and Tyne. The Humber in England is not a river, but an estuary where several rivers merge like the Don, the Ouse and

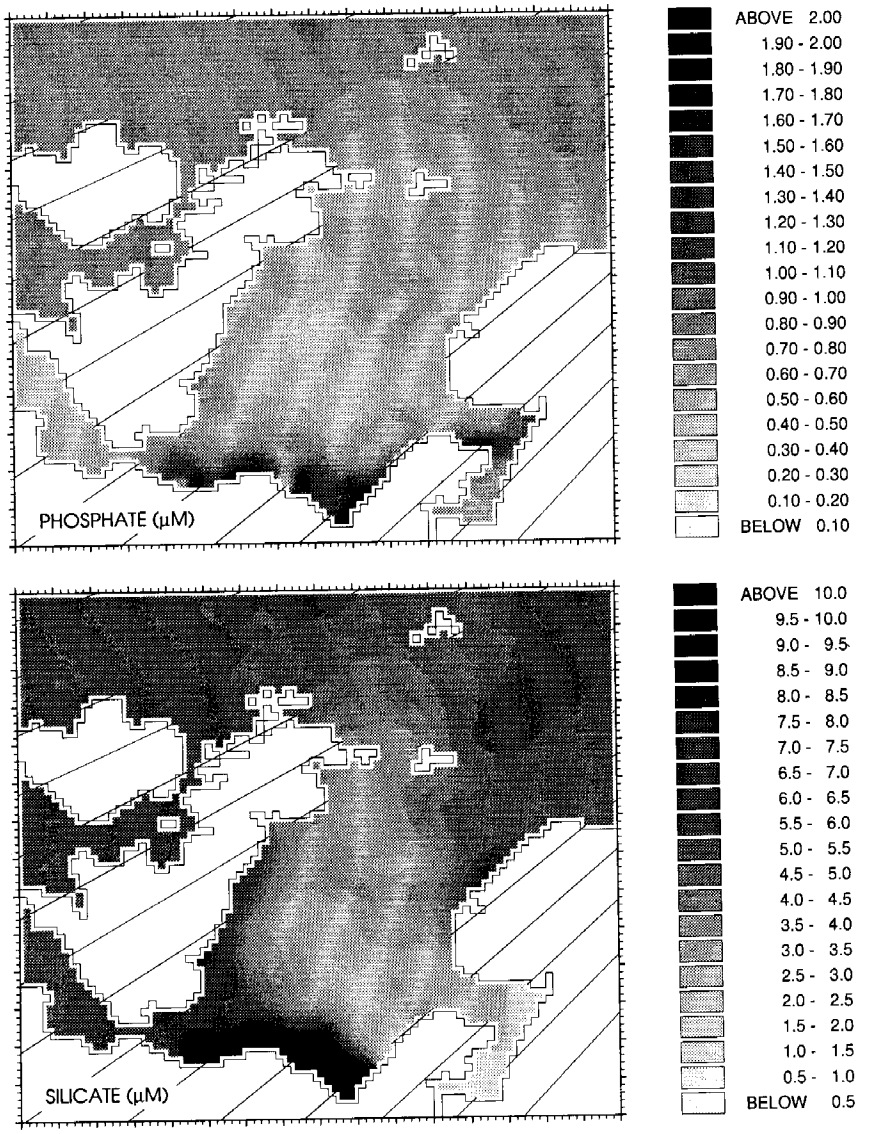

Fig. 10. Concentrations (μM) of phosphate and silicate at 5 m depth in February 1988. These data are used to initialise the simulation model. The nitrate initialisation field are given in Fig. 13. (Data are obtained from ICES).

the Trent. Daily flows have been provided for most of the rivers, but for the Norwegian river Glomma, the Swedish river Bäveån and the Belgian river Scheldt the less frequent data were interpolated linearly. The nutrient concentrations were

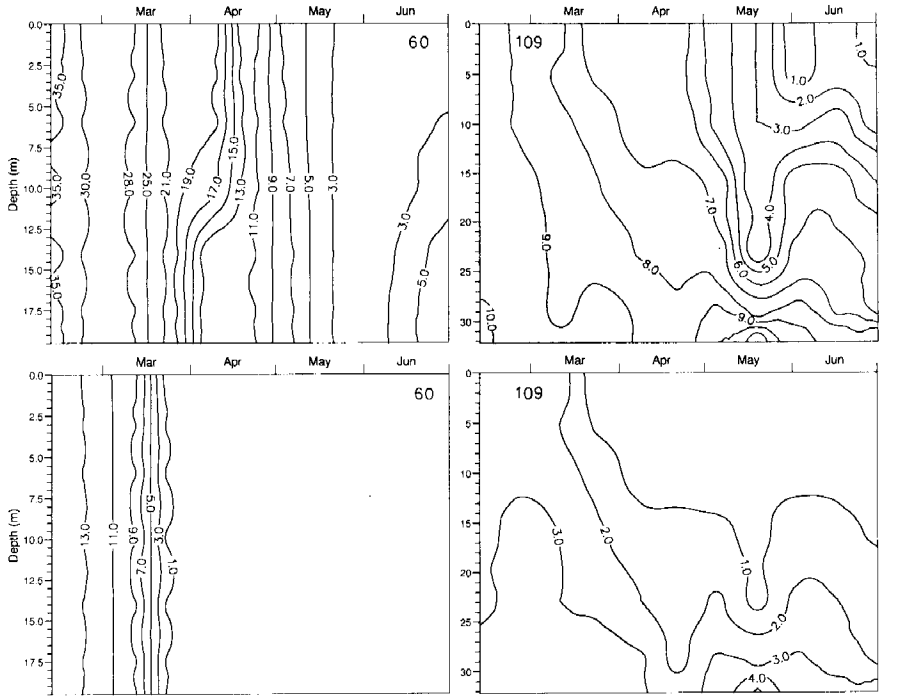

Fig. 11. Simulated vertical profiles of nitrate (upper) and silicate (lower) concentrations during spring 1988 west (Station 60) and east (Station 109) of Denmark. The locations of the stations are given in Fig. 3.

usually given as monthly means, but some countries provided with more frequent observations. The measured parameters were nitrite, nitrate, ammonium, phosphate, silicate, total nitrogen and total phosphate. During the simulation nitrate/ammonium and inorganic phosphate are added into the nitrogen and phosphorus state variables respectively according to the river flow. Organic nitrogen compounds are added to a "detritus" state variable which is being degraded into inorganic nitrogen nutrients as a constant rate ($1.2\ 10^{-7}\ s^{-1}$).

The flagellates and diatoms were homogeneously initialised with a value corresponding to 0.1 mg Chl. *a* m^{-3}. This initial concentration was kept constant until enough light provided net diurnal growth in the surface layers and at this time the death rate and metabolic losses become activated.

Results from the simulation with anthropogenic nutrient input to the North Sea in spring 1988

The initial nutrient data on first of February 1988 are characterised by high

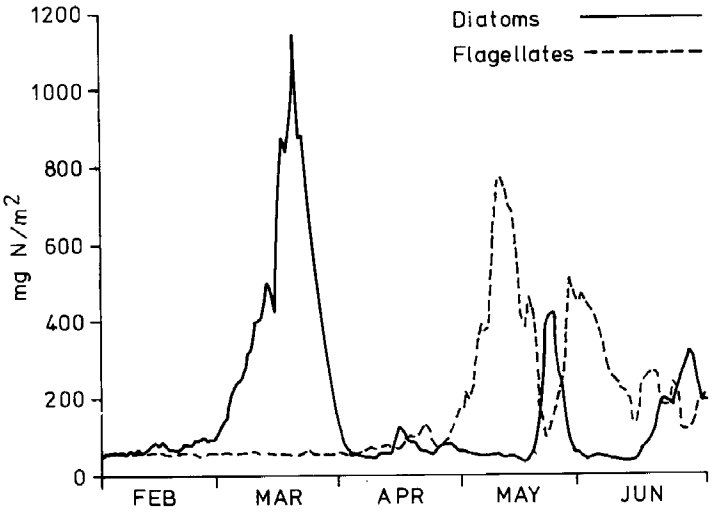

Fig. 12. Simulated diatom and flagellate biomass (mg N m^{-2}) west of Denmark during spring 1988 (Station 60, location is given in Fig. 3).

nutrient concentrations along the coastal areas in the southern and eastern part of the North Sea, while the central part is characterised by low concentrations reflecting a water mass being utilised by phytoplankton the previous year (Fig. 10).

The simulated time evolution of the vertical distribution of nitrate and silicate east and west of Jutland (Denmark) are shown in Fig. 11. West of Denmark (station 60, location indicated in Fig. 3), the simulated distributions of nitrate and silicate indicate a well-mixed water column, while in the Kattegat area (station 109, location indicated in Fig. 3), the simulated water mass was stratified with increasing nutrient concentrations with increasing depth (Fig. 11). These features are also indicated by the April observations given in Fig. 2. The simulation indicates a large diatom bloom west of Denmark (station 60, Fig. 12) during March, and two much smaller blooms in March and April in Kattegat (station 109, Fig. 13). The much lower initial silicate concentrations in the Kattegat area (Fig. 11) explains this geographical difference in the strength of the diatom blooms. Both west of Denmark and in the Kattegat area, the flagellate group did not bloom until May. Observations reviewed by Maestrini & Granéli (1991) indicate a main diatom bloom (their Fig. 2) during March, and a smaller secondary bloom during April. According to them, the *C. polylepis* bloom during May amounted to about 50-100 10^9 cells m^{-2}, while the model indicates a level on the range 50-200 10^9 cells m^{-2} in the same period. For this comparison we have assumed a nitrogen content of 0.26 pmol $cell^{-1}$ (Dahl et al. 1989). Hence, both the timing of the two

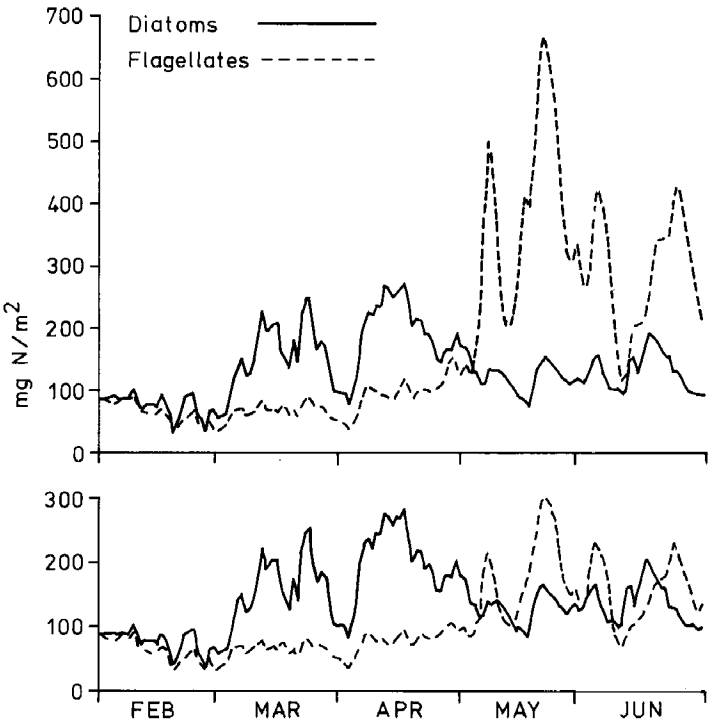

Fig. 13. Simulated diatom and flagellate biomass (mg N m^{-2}) east of Denmark (Station 109, location is given in Fig. 3) during spring 1988 (upper graph). Lower graph is the result from the non-anthropogenic run (see text).

diatom blooms and the timing of the May flagellate bloom are well reflected by the model, but also the magnitude of the flagellate bloom seems to correspond with observations. As demonstrated in Fig. 11 versus 12, however, the simulated strength of the blooms depend strongly on geographical localisation and true quantitative comparisons with the observations reviewed by Maestrini & Granéli (1991) cannot be given.

The simulated diatom bloom in March (Fig. 12) was mainly confined to the coastal areas west of Denmark, with a biomass amounting to 4-6 mg Chl *a* m^{-3} (by assuming a N:Chl a ratio of 10). While the silicate becomes rapidly exhausted (Fig. 11), excessive amounts of nitrate are left over along the western coast of Denmark (Fig. 14, March 16). According to the model these nutrients were utilised by flagellates later on, and during May the nitrate was also exhausted (Fig. 14, May 11).

Simulation without anthropogenic nutrient input to the North Sea

As riverine silicate levels are not severely influenced by human activities the initial data of silicate was equal to those in the anthropogenic run (Fig. 10). The initial nitrate concentrations, however, was reduced in the non-antropogenic run, and were set 1.5 times higher than the silicate concentrations (based on molar concentrations). This corresponds roughly to the N:Si ratio in Atlantic Water. The nitrate to phosphate ratio was assumed equal to the Redfield ratio, and initial phosphate concentrations were set accordingly. The N-nutrient and P-nutrient concentrations in the rivers were reduced by 88% and 80% respectively, while silicate concentrations were kept at the same level as in the anthropogenic run. These values were based on the assumed pristine Rhine conditions as taken from Zobrist and Stumm (1981). All the other forcing of the model such as riverine flow, atmospheric light, wind etc. were the same as in the previous run. Not surprisingly, the diatoms were rather uninfluenced by the altered forcing of the model (Fig. 13) as their growth rate tends to be limited mainly by the unaltered light and silicate conditions. The flagellates, however, were substantially influence by the altered nutrient forcing.

Discussion of the simulation results

Several reports have dealt with general and special aspects of the *C. polylepis* bloom in 1988, see references in Maestrini and Granéli (1991) and Skjoldal & Dundas (1991). Aksnes et al. (1989) and Skjoldal & Dundas (1991) suggest that advection of nutrient loaded water from the southern North Sea into the Skagerrak-Kattegat area may have been important for the mass-development of *C. polylepis*. Such instrusions can be traced by mixing diagrams based on salinity and nitrate of the intermediate and deep water in the Skagerrak-Kattegat area (the water advected from the southern North Sea is more saline and intrudes below the more brackish surface layer in Skagerrak-Kattegat). Thus, upwelling and entrainment processes in the Skagerrak-Kattegat area are believed to fertilise the productive layer with new nutrients having anthropogenic characteristics (high nitrate relative to silicate and phosphate). This mechanism is also considered important by Maestrini & Granéli (1991) as the biomass of *C. polylepis* was frequently higher than the nutrients available in the surface-water pool. To what extent the exceptional bloom was ultimately linked to long-term anthropogenic influence (i.e. eutrophication), however, was questioned by Maestrini & Granéli (1991).

Some important characteristics, however, such as the timing of the different diatom and flagellate blooms (Fig. 2 in Maestrini & Granéli 1991), the different vertical distribution of nutrients west and east of Denmark (Fig. 2) and the early disappearance of silicate relative to nitrate (Fig. 3) are reproduced without any kind of tuning of the model to the actual situation. The present simulations support

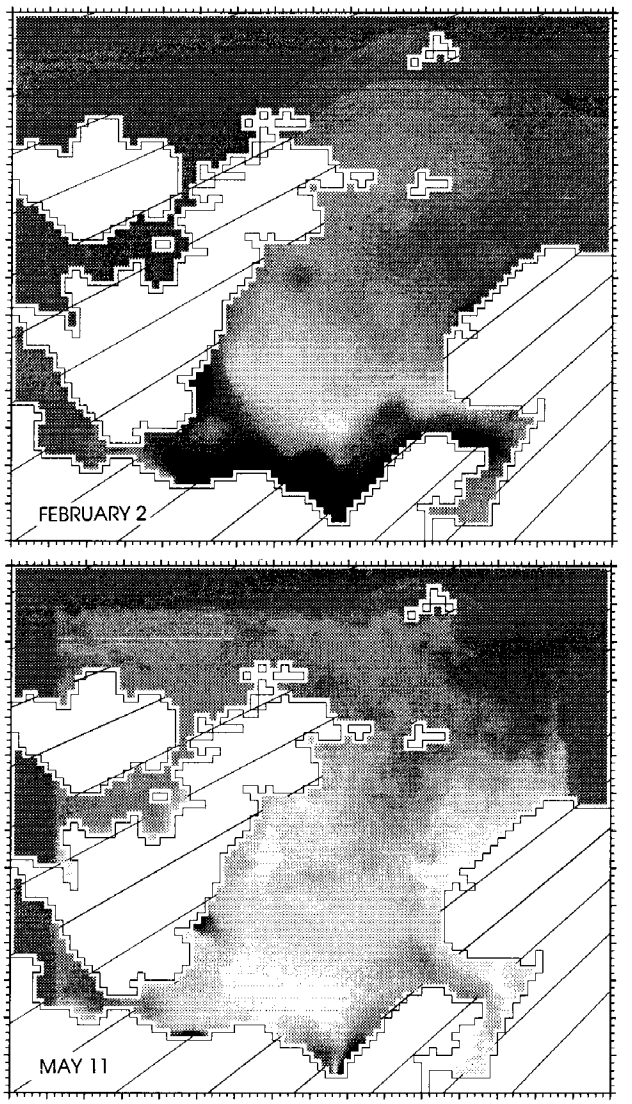

the general idea that flagellates in the North Sea are stimulated by anthropogenic nutrients, but more specifically, also, that a rather strong flagellate bloom in the Kattegat-Skagerrak area was stimulated by such nutrients in May 1988. This corresponds to the timing of the *C. polylepis* bloom, but of course the model cannot tell anything about why the actual species happened to be *C. polylepis* (although it can explain why it could not be a diatom). Such questions should primarily be sought for by a physiological approach including laboratory experiments. The strength of the modelling approach, however, is that it allows for a quantitative in-

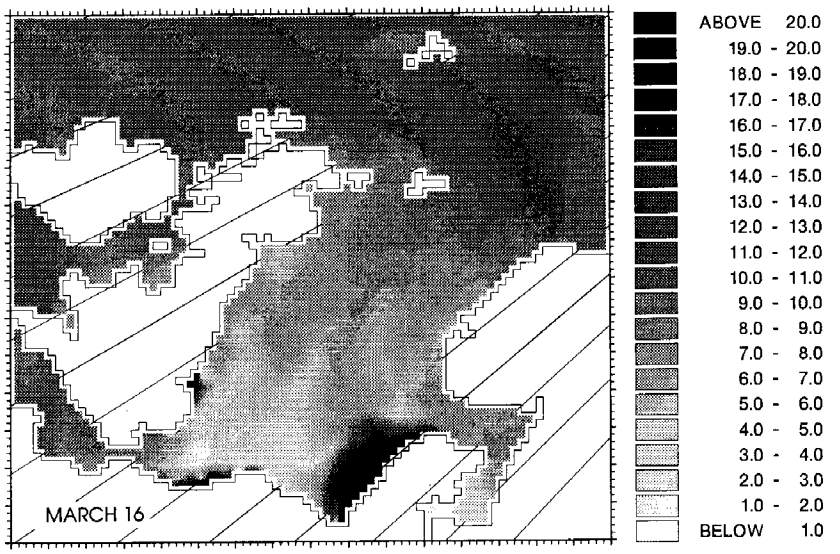

Fig. 14. Simulated horisontal distribution of nitrate (μM) in 5 m depth at selected dates in spring 1988.

tegration of quite complex, although relevant, forcing of the system (such as topography, irradiance, riverine flow, wind etc.) on a temporal and spatial scale that corresponds to the scale of the phenomenon (i.e. the temporal and spatial development of the bloom). Furthermore, sensitivity analysis (in a wide sense) may be performed and provide answers to "what-if" questions. Such an answer is given to the question: "What happens to the phytoplankton if anthropogenic nutrients are removed and the other forcing are unaltered?" is demonstrated in Fig. 13 showing that the peak flagellate concentration in Kattegat was reduced. Hence, it is indicated that the strength of the bloom was influenced by anthropogenic nutrients. This does not mean, however, that the presence of *C. polylepis* is caused by human impact, but rather that this species (and other flagellates as well) is stimulated by present anthropogenic influence. Firstly, because the high anthropogenic N:Si ratio precludes the more rapid growing diatoms from blooming, and secondly because elevated nitrogen and phosphorus concentrations increase the possibility for a higher flagellate mass. Finally, the possible influence of a high anthropogenic N:P ratio on toxicity has also been emphasised (Maestrini & Granéli 1991, Skjoldal & Dundas 1991 and references therein).

The simulations could have been extended to analyse the effect of nutrient reductions in specific countries and rivers, but presently we will not recommend such applications. We do not consider the "story" given by the model as the true story, and this first version of the model has to be improved. A main goal of the

present simulations was to demonstrate the great potential of such models in future environmental management.

CONCLUDING REMARKS

Di Toro et al. (1977) showed that the major features of the regional development of phytoplankton biomass in estuaries can be understood in terms of common equations for growth and environmental limitations. As shown in their simulations of San Francisco Bay and Potomac Estuaries, quite similar kinetic coefficients could be used in order to obtain good fit between observations and model simulations. Thus they concluded that the "kinetic structure" is not necessarily estuary specific but appeared to be applicable in different settings. Their, but also later, studies give a realistic hope that observed nutrient and phytoplankton dynamics may be predicted under different environmental forcing by the use of the same process equations and coefficients (provided that the water movement is well represented). As also pointed out by Di Toro et al. (1977) it is important that the process equations, and their coefficients have a basis in experimental fact, i.e. "within measured ranges". This is perhaps a too weak constraint as measurements within biology and ecology are extremely variable, often conflicting and may be wrong or irrelevant as well. This is due to true natural variability, but also to severe theoretical and methodological shortcomings in ecology. We believe that it is important that the same set of process equations and coefficients are used in several independent applications. It has been a tendency to evaluate simulation models by their ability to fit observations *a posteriori* with reference to the fact that the coefficients were selected within measured ranges. With a multi-coefficient model, however, it is rather easy to provide reasonable fit, and consequently independent validation becomes even more important. Concerning nutrient-phytoplankton dynamics, we think that enclosure (mesocosm) experiments provide ideal validation opportunities for the biological source and sink terms. Partly because the influence of water movement may be eliminated, but also that extreme situations may easily be obtained by manipulations (fertilisation, water renewal, grazing etc.).

For an application model it is not only crucial that the coefficients are based on measurements, but also that the process equations have a theoretical fundament (Loehle 183). Thus, in the development of application models, substitution of purely *descriptive* formulations with *explanatory* formulations (see Platt et al. 1977) may be desirable even if predictive capability is lost in a specific application. The process equations currently used in primary production models are partly descriptive and partly explanatory, and a main goal for quantitative phytoplankton ecology is to establish explanatory formulations. With this aim, progress in the development of ecological simulation models is to be expected.

REFERENCES

Aksnes, D. L., J. Aure, G. K. Furnes, H. R. Skjoldal & R. Sætre, 1989. Analysis of the *Chrysochromulina polylepis* bloom in the Skagerrak, May 1988. Environmental Conditions and Possible Causes. - Bergen Scientific Centre, BSC 89/1, Bergen. 38 pp.

Aksnes, D. L. & J. K. Egge, 1991. A theoretical model for nutrient uptake in phytoplankton. - Mar. Ecol. Prog. Ser. **70**: 65-72.

Aksnes, D. L. & U. Lie, 1991. A coupled physical-biological pelagic model of a shallow sill fjord. - Estuarine, Coastal and Shelf Science **31**: 459-486.

Andersen, V. & P. Nival, 1989. Modelling of phytoplankton dynamics in an enclosed water column. - J. mar. biol. Ass. U.K. **69**: 625-646.

Andersen, V., P. Nival & R. P. Harris, 1987. Modelling of a planktonic ecosystem in an enclosed water column. - J. mar. biol. Ass. U.K. **67**: 407-430.

Anon., 1989. Solar radiation and radiation balance data (The world network). - World Radiation Data Centre. Voeikov Geophysical Observatory. St. Petersburg.

Anon., 1991. Radiation observations in Bergen, Norway 1990. The radiation observatory. Radiation yearbook 26. Meteorological Geophysical Institute. University of Bergen.

Blumberg, A. F. & G. L. Mellor, 1987. A Description of a Three-Dimensional Coastal Ocean Circulation Model. - *In* N. Heaps (ed.): Three-Dimensional Coastal Ocean Models, Vol. 4. American Geophysical Union, Washington D.C.

Bratbak, G., J. K. Egge & M. Heldal, 1993. Viral mortality of the marine alga *Emilania huxleyi* (Hapthophyceae) and termination of algal blooms. - Mar. Ecol. Prog. Ser. **93**: 39-48.

Dahl, E., O. Lindahl, E. Paasche & J. Throndsen, 1989. The *Chrysochromulina polylepis* bloom in Scandinavian waters during spring 1988. - *In* E. M. Cosper, V. M. Briceli & E. J. Carpenter (eds.): Novel phytoplankton blooms: Causes and impacts of recurrent brown tides. Coastal and estuarine studies **35**: 383-405. Springer Verlag. Berlin.

Di Toro, D. M., R. V. Thomann, D. J. O'Connor & J. L. Mancini, 1977. Estuarine phytoplankton biomass models - verification analyses and preliminary applications. - *In* E. D. Goldberg, I. N. McCave, J. J. O'Brien & J. H. Steele (eds.): The Sea. Ideas and Observations on Progress in the Study of the Seas. Volume 6: Marine modelling, pp. 969-1020. John Wiley & Sons. New York.

Egge, J. & D. L. Aksnes, 1992. Silicate as regulating nutrient in phytoplankton competition. - Mar. Ecol. Prog. Ser. **83**: 281-289.

Eppley, R. W., 1972. Temperature and phytoplankton growth in the sea. - Fishery Bulletin **70**: 1063-1085.

Furnas, M. J., 1990. *In situ* growth rates of marine phytoplankton: approaches to measurement, community and species growth rate. - J. Plankton Res. **12**: 1117-1151.

Jørgensen, S. E., L. Kamp-Nielsen, T. Christensen, J. Windolf-Nielsen & B. Westergaard, 1986. Validation of a prognosis based upon a eutrophication model. - Ecol. Modelling **32**: 165-182.

Kremer, J. N. & S. W. Nixon, 1978. A Coastal Marine Ecosystem. Simulation and analysis. - Springer-Verlag. Berlin. 211 pp.

Langdon, C., 1988. On the causes of interspecific differences in the growth-irradiance relationship for phytoplankton. II. A general review. - J. Plankton Res. **10**: 1291-1312.

Lehman, R., 1988. On a simple flux-corrected transport algorithm for the solution of the advection-diffusion equation in the case of predominant advection. - Z. Meteorol. **38**: 299-307.

Levitus, S., 1982. Climatological atlas of the World Ocean. - NOAA Prof. Pap. **13**, 173 pp.

Loehle, C., 1983. Evaluation of theories and calculation tools in ecology. - Ecol. Modelling **19**: 239-247.

Maestrini, S. E. & E. Granéli, 1991. Environmental conditions and ecophysiological mechanisms which led to the 1988 *Chrysochromulina polylepis* bloom: an hypothesis. - Oceanologica Acta **14**: 397-413.

Martinsen, E. A. & H. Engedahl, 1987. Implementation and testing of a lateral boundary scheme as an open boundary condition in a barotropic ocean model. - Coastal Engineering **11**: 603-627.

Nelisson, P. H. M. & J. Stefels, 1988. Eutrophication in the North Sea. - NIOZ-Report **4**, Nederlands Instituut Ondersoek der Zee.

Officer, C. B. & J. H. Ryther, 1980. The possible importance of silicon in marine eutrophication. - Mar. Ecol. Prog. Ser. **3**: 83-91.

Ottersen, G., 1991. MODgrid a model oriented data grider. - Internal report at the Institute of Marine Research, Bergen.

Peters, J. C. H. & P. Eilers, 1978. The relationship between light intensity and photosynthesis. A simple mathematical model. - Hydrobiological Bulletin **12**: 134-136.

Platt, T., K. L. Denman & A. D. Jassby, 1977. Modelling the productivity of phytoplankton. - *In* E. D. Goldberg, I. N. McCave, J. J. O'Brien & J. H. Steele (eds.): The Sea. Ideas and Observations on Progress in the Study of the Seas. Volume 6: Marine modelling, pp. 807-856. John Wiley & Sons. New York.

Sathyendranath, S. & T. Platt, 1990. The light field in the ocean: its modification and exploitation by the pelagic biota. - *In* P. J. Herring (ed.): Light and Life in the Sea, pp. 333-344. Cambridge University Press.

Skartveit, A. & J. A. Olseth, 1986. Modelling slope irradiance at high latitudes. - Solar Energy **36**: 333-344.

Skjoldal, H. R. & I. Dundas, 1991. The *Chrysochromulina polylepis* bloom in the Skagerrak and the Kattegat in May-June 1988: Environmental conditions, possible causes, and effects. - ICES cooperative research report no. **175**. International Council for the Exploration of the Sea, Copenhagen. 59 pp.

Skogen, M. D., E. Svendsen, J. Berntsen, D. L. Aksnes & K. B. Ulvestad, in press. Modelling the Primary Production in the North Sea using a coupled 3-dimensional physical-biological ocean model. - Coastal, Estuarine and Shelf Science.

Ziljstra, J. J., 1988. The North Sea Ecosystem. - *In* H. Postma & J. J. Ziljstra (eds.): Ecosystem of the world **27**: Continental shelves, 231-274. Elsevier. Amsterdam. 421 pp..

Zobrist, J. & W. Stumm, 1981. Chemical dynamics of the Rhine catchment area in Switzerland, extrapolation to "pristine" Rhine river input to the ocean. - *In* River Inputs to Ocean Systems, pp. 52-63. United Nations, New York. 384 pp.